MINERALOGICAL MAGAZINE, JUNE 1970, VOL. 37, NO. 290

Pyroxenes from non-carbonaceous chondritic meteorites

R. A. BINNS

Department of Geology, University of New England, Armidale, New South Wales, Australia

SUMMARY. Chemical, optical, and X-ray data are presented for pyroxenes from a representative selection of chondrites. The Mg–Fe pyroxenes originally crystallized above 1000–1200 °C as the protoenstatite–protohypersthene polymorph, and inverted on cooling to the polysynthetically twinned clinoenstatite–clinohypersthene polymorph. In most chondrites the latter became converted to orthopyroxene during recrystallization at temperatures ranging up to 900 to 950 °C. The contents of certain minor elements changed during the clino–ortho inversion. Ancestral protoenstatite–protohypersthene may have been slightly non-stoichiometric. Accessory Ca-rich pyroxenes are discussed briefly.

RECENT studies, directed towards large collections rather than single individuals, have led to greatly improved petrographic and genetic understandings of chondritic meteorites. By providing a more satisfactory basis for the selection of representative material than existed in the past, these advances have stimulated a new investigation of major constituents in a number of chondrites from the extensive collections of the British Museum (Natural History), London. Of the several mineral groups examined, it is appropriate to discuss the pyroxenes separately, for, as indicated by the following paragraphs, they bear interesting genetic implications and are also important to chondrite classification.

Most non-carbonaceous chondrites contain Ca-poor pyroxene in the orthorhombic modification, and are 'equilibrated' in the sense that their ferromagnesian silicates are remarkably homogeneous in composition (Keil and Fredriksson, 1964). The overall oxidation state of such stones is specified by the Fe/Mg ratio of either their olivine or pyroxene (Prior, 1920; Mason, 1962, 1963, 1967*a*). The tendency among known representatives for oxidation states to cluster within several narrow and generally well-separated intervals permits a simple and most useful means of classification, the nomenclature of which is based in part on pyroxene composition. Currently recognized non-carbonaceous chemical-mineralogical groupings include *enstatite chondrites* ($Fs_{\approx 0}$), *olivine–bronzite chondrites* (Fs_{15-18}), *olivine–hypersthene chondrites* (Fs_{20-23}), and amphoteric chondrites or *amphoterites* (Fs_{25-27}), where the figures in parenthesis represent the approximate ranges in mol % ferrosilite in constituent pyroxene.[1]

[1] The pyroxene subdivision employed by Prior (1920)—namely enstatite, Fs_{0-10}; bronzite, Fs_{10-20}; hypersthene, Fs_{20-50}—is firmly established in the meteoritical literature. Its correspondence to the hiatus between olivine–bronzite and olivine–hypersthene chondrites is improved if $MnSiO_3$ is allocated to 'ferrosilite'. No satisfactory pyroxene name is available for the amphoterites, which are included by some workers in the olivine–hypersthene chondrites.

A comparatively small number of essentially non-carbonaceous chondrites, the 'unequilibrated chondrites' of Dodd and Van Schmus (1965), are characterized in part by possession of monoclinic rather than orthorhombic Ca-poor pyroxene and by compositionally inhomogeneous ferromagnesian silicates, and cannot be classified on the basis of pyroxene compositions in this way because of a less regular distribution of Fe between their constituents. However, bulk chemical criteria suggest that these fall into the same major categories as their 'equilibrated' analogues. For the purposes of this article the chemical subdivision of non-carbonaceous chondrites into E, H, L, and LL groups (cf. Urey and Craig, 1953; Keil and Fredriksson, 1964; Van Schmus and Wood, 1967) may be treated as the equivalent of the mineralogical classification listed above.

The relationship between unequilibrated and equilibrated chondrites is at present a much-disputed question, too lengthy to be discussed in full here. It will be sufficient to note that the mineralogical distinction (based on symmetry of pyroxene, and homogeneity or otherwise of pyroxene and olivine) is paralleled by variations in textural characteristics, and that the range in properties found within each chemical-mineralogical class of chondrite has been widely interpreted as a reflection of varied degrees of post-accumulation recrystallization (cf. especially Van Schmus and Wood, 1967; Binns, 1967*a*; Dodd, 1969). According to this interpretation unequilibrated chondrites are thought to have largely avoided recrystallization, and to represent the kind of material from which equilibrated varieties were derived. The concept underlies the selection of material and much of the discussion in the present article, and also forms the basis for nomenclature used in a previous attempt to subdivide the chondrite textural range into Primitive, Transitional, and Recrystallized Groups (Binns, 1967*a*).[1] Genetic implications are avoided in the nomenclature of an alternative textural subdivision (with different 'boundaries') by Van Schmus and Wood (1967), who erected six 'petrologic types' of which four (Types 3–6) are applicable to non-carbonaceous chondrites. Pyroxene relationships discussed below lend much support to the recrystallization concept.

Meteorites studied. Table I lists relevant details of seven meteorites from which pyroxene concentrates were obtained. Except that there is no highly primitive olivine-bronzite chondrite, these represent the extreme textural types for each of the non-carbonaceous chemical-mineralogical classes. The four recrystallized chondrites are known to be essentially 'equilibrated', either from electron probe data in the literature or from new measurements by the author. Château-Renard is veined and contains shock-produced maskelynite rather than plagioclase.

The unequilibrated character of the three primitive chondrites has been established by electron-probe measurements showing variable compositions in olivine and pyroxene, and is supported for Kota-Kota by coexistence of accessory olivine with

[1] In a development of this classification (Binns, in preparation), the former is separated into a subgroup of chondrites retaining some primary chondrule glass (highly primitive or 'glassy-primitive' chondrites—usually unequilibrated) and one comprising stones with well-preserved chondritic structures but in which all former chondrule glass has become devitrified ('devitrified-primitive' chondrites—usually equilibrated or almost so). This further subdivision is employed in the text.

traces of quartz, tridymite, and cristobalite (Binns, 1967*b*). However, the restricted range of olivine compositions in Ghubara indicates a state approaching equilibration (% mean deviation in Fe content of olivine = 4·4, compared with 19 for Parnallee). This is a xenolithic stone (Binns, 1968), of which the dark host portion was used to obtain the pyroxene concentrate. Its classification as H4 by Van Schmus and Wood

TABLE I. *Details of meteorites studied*

Name	B.M. number	Class	Type*	Olivine Composition (mol. % fayalite)
Recrystallized Group chondrites†				
Hvittis	86754	Enstatite	E6	absent
Oakley	84814	Olivine–bronzite	H6	19
Château-Renard	16355	Olivine–hypersthene	L6	25
Appley Bridge	1920,40	Amphoterite	LL6	30
Glassy-Primitive Group chondrites†				
Kota-Kota	1905,355	Enstatite	E3	0·3–1·9
Ghubara (host)	1954,207	Olivine–hypersthene	L3–L4	22–27
Parnallee	34792	Amphoterite	LL3	0–44

* After Van Schmus and Wood (1967), and see text.
† After Binns (1967*a*).

(1967) probably refers to B.M. 1962,133, formerly included among the Ghubara stones but now known as *Jiddat al Harasis* (M. H. Hey, pers. comm.; cf. Mason, 1967*a*). Judging from the range in olivine compositions and the comparative scarcity of fresh glass, the host portion of Ghubara is intermediate between types L3 and L4.

Kota-Kota contains sharply defined chondrules with some pale isotropic violet-brown glass, a dark inter-chondrule mesostasis, and a mean deviation in Fe content of olivine of approximately 35 %. These features suggest that it is more appropriately classified as an E3 chondrite, as listed in Table I, rather than E4 as given by Van Schmus and Wood (1967).

Three additional recrystallized stones are listed in table IV. Moti-ka-nagla (B.M. 43332) is an olivine–bronzite chondrite; Peetz (B.M. 1938,1205) and Tauq (B.M. 1936,151) are olivine–hypersthene chondrites.

Separation and analytical techniques. The Ca-poor pyroxene concentrates were obtained from crushed samples by repeated heavy-liquid separation, after extraction of metal with a hand magnet. The provisional concentrates were reground at each stage, dust being removed with the aid of an ultrasonic disintegrator. Fresh Clerici solution and, in the final stages, miniature centrifuge tubes were used. Up to five operations were required to achieve satisfactory purity and the yield was poor: *c.* 0·5–1 g of final concentrate (approx. 10–20 μm grain-size) were obtained from meteorite samples ranging from 150 g of the amphoterites to 18 g of Hvittis and 2 g of Kota-Kota. To avoid possible preferential leaching no attempt was made to extract olivine, the most problematical contaminant, by solution in hydrochloric acid.

However, brief treatment with 1:10 HCl followed by Na_2CO_3 solution and thorough washing was employed in the earlier stages to remove brown oxide coatings.

Final purity of the Hvittis, Kota-Kota, and Appley Bridge concentrates exceeded 99·5 %, and that of the Château-Renard pyroxene was close to 99·5 %, the principal contaminants being tiny opaque and low-refractive-index inclusions. Comparable amounts of similar inclusions remained in the Ghubara and Parnallee concentrates, but these and the Oakley pyroxene were also contaminated with the quantities of olivine listed in table II (estimated by grain counts and confirmed where more abundant by the intensities of the olivine 130 peaks on diffractometer traces). The nature of the low-refractive-index inclusions is uncertain; in the clinopyroxenes particularly these tend to be vermicular in appearance and may be either feldspar, glass, or even open cavities. The Oakley concentrate contained the highest opaque impurity (0·1–0·2 %).

Microanalyses were performed on *c.* 300 mg samples divided into three portions. From an Na_2CO_3 fusion of the first, SiO_2 was determined by standard gravimetric methods, following which iron was extracted from a redissolved R_2O_3 precipitate with isopropyl ether (Moss *et al.*, 1961) before determining Al_2O_3 as the 8-hydroxyquinoline complex (Riley, 1958). MgO was then determined gravimetrically as pyrophosphate, and nickel was measured spectrophotometrically as Ni dimethylglyoxime after extraction by chloroform from the Mg filtrate (Libermann, 1955). From a 'solution B' (Shapiro and Brannock, 1962) of the second portion, total iron, MnO, Cr_2O_3, P_2O_5, and TiO_2 were determined spectrophotometrically as sulphosalicylic complex (Thiel and Peter, 1935), permanganate, diphenylcarbazide complex, reduced blue molybdate complex, and tiron complex (after extraction of Fe with isopropyl ether) respectively, and CaO, Na_2O, and K_2O were measured by flame photometer using a standard addition technique. The third portion was digested under N_2 in H_2SO_4–HF and used to measure FeO spectrophotometrically as the ferrous dipyridyl complex (Riley and Williams, 1959), after which ferric iron was determined by reducing with solid hydroxylamine hydrochloride and measuring the increase in absorbance. Wherever possible, dilutions permitting maximum sensitivity in instrumental measurements were chosen by reference to optical and literature data, or if necessary by undertaking preliminary determinations on less pure mineral concentrates.

Optical and X-ray measurements. All refractive indices were determined on the analysed powders by the immersion method at 25 ± 1 °C using Na light, mixtures of closely spaced liquids, and a carefully calibrated Abbé refractometer. For orthopyroxenes, γ was measured along the {210} cleavage, β on optic axis sections, and α taken as the minimum value observed. No significant variation in γ could be detected, confirming the homogeneity of these samples. Measurements on the monoclinic pyroxenes were hindered by fine polysynthetic twinning and compositional inhomogeneity. The extent of the latter is indicated by the following ranges from α min to γ max, compared to the low birefringence: Kota-Kota, 1·652–1·665; Parnallee, 1·655–1·695; Ghubara, 1·673–1·692. Fortunately, the more extreme values were rare

and there appeared to be a pronounced compositional mode in each sample. The powders were successively immersed in oils at 0·002 intervals and numerous measurements made as follows: γ and β were taken as the two vibration directions of grains showing sharply defined vertical (100) twin planes and relatively high birefringence, and α was measured across (010) grains showing straight extinction and no apparent twinning. The refractive indices for clinopyroxenes quoted in table II represent average modal values.

Reference X-ray powder patterns (table III) were obtained with smear mounts of the analysed powders, using a Philips 1011 diffractometer run in both directions at $\frac{1}{4}^\circ$ per minute. Peaks were calibrated against the stronger reflections from separate mounts mixed with silicon or quartz internal standards. For cell dimension measurements, from six to eight scans over appropriate ranges were made of both sample and sample plus standard mounts at the following conditions: Ni filtered Cu radiation; scan speed $\frac{1}{8}^\circ$ 2θ per minute; chart $2'' = 1^\circ$ 2θ; time constant 8 sec; receiving slit, $0{\cdot}1^\circ$; scatter and divergent slits, 1°; with pulse height analysis. Preliminary cell dimensions for the Hvittis and Kota-Kota pyroxenes were calculated from unambiguous low-angle reflections, and the indices of all peaks then checked using this data against the patterns listed by Smith *et al.* (1969) for orthoenstatite and by Stephenson *et al.* (1965) for clinoenstatite. Although intensities (measured as area below peaks) varied slightly, the correspondence in patterns was excellent, the only important difference being the presence of a reflection here indexed as 531 in clinoenstatite. This latter was also present in the pattern of a synthetic clinoenstatite supplied by Tem-Pres Research Inc. Final cell dimensions were obtained by least squares reduction of from 15 to 21 good reflections, using an IBM 1620 program adapted from that of Burnham (1962). Weighting was generally based on the standard deviation in 2θ measurements, but also took account of apparent asymmetry in certain peaks. For the Ghubara clinopyroxene, reflections that do not seriously conflict with orthopyroxene peaks were most favourably weighted.

Orthopyroxenes

Chemistry. Data presented in table II show the Hvittis orthopyroxene to be almost pure enstatite, with Ca, Fe, and Al as the only minor components of any significance. The other three orthopyroxenes contain variable Fe″, minor Ca and Mn, and comparatively low Al, Ti, and Cr. Ferric iron is absent or virtually lacking, that detected in Hvittis being probably due to terrestrial oxidation.

The listed Ni contents might arise partly from metal impurities in the samples, but except in the Hvittis enstatite (30 ppm Ni), the quantities of contaminant needed to provide 150–200 ppm Ni (approximately 0·1 wt %, based on separate analyses of bulk metal samples from each stone) exceed the amount of opaque material visible in the concentrates. Unless the contaminant is exclusively taenite, it appears that at least some Ni is contained within the pyroxenes. Corrections to the Fe/Mg ratios of the analysed pyroxenes, assuming all Ni to be present in metal, are in any event negligible (see table II).

TABLES II *and* III (*opposite*) *Chemical, optical, and X-ray data for chondritic Mg–Fe pyroxenes; anal. A. J. Easton*

	Orthopyroxene				Clinopyroxene		
	Hvittis	Oakley	Château-Renard	Appley Bridge	Kota-Kota	Parnallee	Ghubara
SiO_2	59·0	54·7	55·4	54·5	58·2	55·2	54·6
TiO_2	< 0·03	0·19	0·19	0·19	0·03	0·10	0·15
Al_2O_3	0·33	0·22	0·35	0·29	0·32	0·71	0·54
Cr_2O_3	< 0·06	0·15	0·18	0·11	0·36	0·60	0·39
Fe_2O_3	0·03	< 0·1	< 0·1	< 0·1	0·03	< 0·1	< 0·1
FeO	0·23	11·1	13·4	16·0	0·93	8·5	12·6
MnO	< 0·1	0·54	0·48	0·45	0·1	0·42	0·47
MgO	39·1	31·6	28·9	27·0	39·5	32·8	29·7
NiO	0·004	0·026	0·025	0·019	0·034	0·022	0·027
CaO	1·0	1·0	0·9	1·0	0·4	1·3	1·4
Na_2O	0·02	0·06	0·08	0·03	0·05	0·14	0·21
K_2O	0·02	0·005	0·005	0·005	0·005	0·01	0·03
P_2O_5	< 0·1	< 0·1	< 0·1	< 0·1	< 0·1	< 0·1	< 0·1
Total	99·7	99·6	99·9	99·6	100·0	99·8	100·1
Cation contents (*6 oxygen atoms*)							
Si	1·987	1·951	1·983	1·982	1·966	1·943	1·952
Al	0·013	0·009	0·015	0·012	0·013	0·030	0·023
Ti	0·000	0·005	0·005	0·005	0·001	0·003	0·004
Cr	0·000	0·004	0·005	0·003	0·010	0·016	0·011
Fe^{2+}	0·007	0·331	0·401	0·486	0·027	0·250	0·377
Mn	0·000	0·016	0·015	0·014	0·003	0·012	0·014
Mg	1·962	1·679	1·541	1·462	1·987	1·719	1·582
Ni	0·000	0·001	0·001	0·001	0·001	0·001	0·001
Ca	0·036	0·038	0·034	0·039	0·014	0·049	0·054
Na	0·001	0·004	0·006	0·002	0·003	0·010	0·015
K	0·001	0·000	0·000	0·000	0·000	0·000	0·001
Z	2·000	1·960	1·998	1·994	1·979	1·973	1·975
$X+Y$	2·007	2·078	2·008	2·012	2·046	2·060	2·059
$\frac{100(Fe+Mn)}{Fe+Mn+Mg}$	0·37	17·1	21·2	25·5	1·48	13·2	19·8
$100Fe/(Fe+Mg)$	0·37	16·5	20·6	25·0	1·34	12·7	19·2
$100Fe^*/(Fe^*+Mg)$	0·33	16·4	20·5	25·0	0·52	12·6	18·9
Impurities							
% olivine	0	2	0·2	< 0·1	< 0·1	1	1
Optical properties							
α	$1·653_5$	$1·673_5$	1·677	1·682	1·654	1·668	1·675
β	$1·655_5$	1·680	1·685	1·691	1·656	1·671	1·678
γ	$1·662_5$	$1·684_5$	$1·689_5$	$1·695_0$	1·663	1·681	1·688
2V (calc.)	+56	−79	−74	−67	+56	+57	+57
γ: [001] (±2°)	—	—	—	—	24	33	36
Cell dimensions							
a	18·243 Å	18·267	18·275	18·287	9·602	9·618	9·623
b	8·820	8·856	8·871	8·878	8·822	8·842	8·864
c	5·187	5·204	5·201	5·211	5·169	5·182	5·185
β	—	—	—	—	108·19° (±0·03)	108·36 (±0·04)	108·24 (±0·15)
V	834·6 Å^3	841·8	843·1	846·0	416·0	418·2	420·1

* Corrected values for Fe assuming all Ni is contained in metallic impurity.

	Orthopyroxene				Clinopyroxene				
	Hvittis		Appley Bridge		Kota-Kota			Parnallee	
hkl	*d*	I/I_0	*d*	I/I_0	*hkl*	*d*	I/I_0	*d*	I/I_0
210	6·344 Å	1	—	—	110	6·350 Å	1	—	—
400	—	—	4·558 Å	6	020	4·410	7	4·418 Å	4
020	4·413	10	4·439	4	011	4·291	2	4·301	1
211	—	—	4·040	9	210	4·045	1	—	—
121	3·305	11	3·324	15	021	3·286	20	3·287	15
420	3·170	135	3·182	165	220	3·171	70	3·177	85
221	3·152				22$\bar{1}$	2·975	45	2·982	55
321	2·942	19	2·957	36	310	2·875	100	2·880	100
610	2·876	100	2·884	100	130	2·799	1	—	—
511	2·828	7	2·837	18	13$\bar{1}$	2·532	20	2·542	40
230	2·799	< 1	—	—	20$\bar{2}$			2·519	2
421	2·706	14	2·718	18	002	2·455	20	2·459	35
131	2·534	19	2·549	38	221	2·434	10	2·436	10
611	—	—	2·524	< 1	23$\bar{1}$	2·375	4	2·381	2
202	2·494	9	2·505	7	400	2·280	3	—	—
521	2·471	12	2·481	25	102	2·208	3	2·210	6
302	—	—	2·395	2	040				
331	2·357	3	—	—	112	2·136	< 1	—	—
800	2·281	2	—	—	33$\bar{1}$	2·115	10	2·119	20
402	2·255	3	2·259	3	42$\bar{1}$	2·094	2	2·096	4
431	2·231	2	2·243	1	420	2·027	≪ 1	2·023	15
630	2·114	8	2·122	15	40$\bar{2}$	2·014	5		
531	2·095	9	2·106	23	041				
721	2·058	5	2·066	7	240	1·984	4	1·987	4
820	2·030	< 1	2·032	15	24$\bar{1}$	1·934	3	1·940	1
141	2·017	1			43$\bar{1}$	1·848	≪ 1	—	—
440	1·985	2	1·995	15	510	1·786	6	1·789	5
241	1·981	3			222	1·770	≪ 1	—	—
631	1·957	9	1·966	20	241	1·762	2	1·765	2
821	1·887	2	1·894	5	52$\bar{1}$				
10,10	1·787	4	1·792	4	150	1·732	5	1·736	5
541	1·774	2	1·786	3	312	1·642	1	1·641	< 1
250	1·732	4	1·744	14	53$\bar{1}$	1·606	10	1·608	25
831	1·702	3	1·706	5	341	1·586	2	1·591	< 1
812			1·687	< 1	440				
023	1·607	2	1·617	2	350	1·527	1	1·530	3
10.2.1					600	1·521	9	1·522	7
413	1·589	2	1·596	7	23$\bar{3}$	1·484	1	1·488	2
931					060	1·470	6	1·474	15
840	1·585	2			402	1·467	2	—	—
650	1·526	4	1·534	6	52$\bar{3}$	—	—	1·395	1
12.0.0	1·520	6	1·524	9	531	1·377	10	1·378	15
10.3.1	1·485	11	1·490	28	133	1·357	1	—	—
060	1·470	12	1·479	24	24$\bar{3}$				
352	—	—	1·427	2	710	1·290	1	—	—
11.0.2	1·397	< 1	1·414	< 1	26$\bar{2}$	1·269	1	1·268	2
11.3.1	1·391	8	1·396	21	062	1·262	≪ 1		
12.3.1	1·307	2	1·311	8	35$\bar{3}$	1·215	< 1	1·216	< 1
12.1.2	1·297	< 1	1·301	4	352				
14.1.0	1·290	< 1	—	—	28$\bar{1}$	1·064	≪ 1	—	—
214	1·267	2	1·274	7	66$\bar{2}$	1·057	≪ 1	—	—
10.5.0					750	1·049	2	1·050	1
304									
14.5.0	1·048	5	1·053	2					

The effects of possible feldspar impurities are also small, and the low $Na_2O:Al_2O_3$ in the analyses indicates that most of the reported Al is a genuine minor component of the pyroxenes. Apart from that of the Oakley concentrate, which is the most highly contaminated by olivine and non-magnetic opaques, the analyses recalculate well to metasilicate formulae. Although detailed consideration of minor element substitution is scarcely justified, it may be noted that satisfactory charge balance is obtained by assuming small $NaCrSi_2O_6$ (cosmochlore) and $CaTiAl_2O_6$ components. Only in the Hvittis enstatite is Al apparently shared between the four-fold and six-fold co-ordination sites.

Optical properties. Fig. 1 shows a near-ideal linear dependence of the γ and α refractive indices on Fe+Mn content. These are systematically 0·004 higher than interpolated values for synthetic Fe–Mg orthopyroxenes, and slightly lower than those of typical terrestrial orthopyroxenes with similar Fe contents (lines A and B respectively, fig. 1). The latter tend to be richer in Ca and Al than chondritic orthopyroxenes, but although Deer *et al.* (1963) suggest that Ca has little influence on refractive index, this component appears the most likely explanation of the difference between the synthetic and chondritic orthopyroxenes in view of the low Al_2O_3 values reported in table II. The calculated optic axial angles of the chondritic orthopyroxenes agree with those of terrestrial equivalents.

Since orthopyroxene γ is rapidly and accurately measurable in crushed samples, the correlation in fig. 1 provides a simple optical method for classifying a recrystallized chondritic meteorite. The values 1·687 and 1·693 respectively divide olivine–bronzite from olivine–hypersthene chondrites, and olivine–hypersthene chondrites from amphoterites. Diagrams based on terrestrial pyroxenes are not satisfactory for this purpose.

Most chondritic orthopyroxenes give comparatively sharp extinction between crossed polars, although in some less thoroughly recrystallized chondrites there may be a striated appearance evidently due to relic twinning (discussed further below). The {210} cleavage is not usually pronounced in thin section, but becomes moderately well developed in crushed samples. However, the Château-Renard orthopyroxene is anomalous. It shows only a very poor cleavage in the crush, and has an irregular extinction of the type reported from brecciated enstatite achondrites (Reid and Cohen, 1967).

Cell dimensions. As shown in fig. 2, cell dimensions of the chondritic orthopyroxenes also vary systematically with Fe+Mn content. The greatest variation is in *b*, which also conforms most closely to interpolated values for synthetic equivalents, but cell volume, *c*, and to a lesser extent *a* are consistently higher. Although evidence of Mg–Fe site preference in terrestrial orthopyroxenes (Smith *et al.*, 1969; see also Dundon and Walter, 1967) introduces some uncertainty into the significance of the dashed lines in fig. 2, there is nevertheless an apparent increase in cell dimensions and cell volume due to Ca content in chondritic orthopyroxenes (cf. Hess, 1952; Deer *et al.*, 1953).

Because of their uniform Ca and low Al contents (see Zwaan, 1954; Boyd and England, 1960), the angular spacing between the 10.3.1 and 610 peaks gives a comparatively accurate measure of pyroxene composition for recrystallized chondrites (fig. 3). Since olivine interferes with the 10.3.1 peak, it is necessary first to treat the sample with HCl. With care, a precision of ± 1 mol % 'ferrosilite' is obtainable. The values 0·58° and 0·55° mark the boundaries between the olivine–bronzite olivine–hypersthene, and amphoterite chondrite classes.

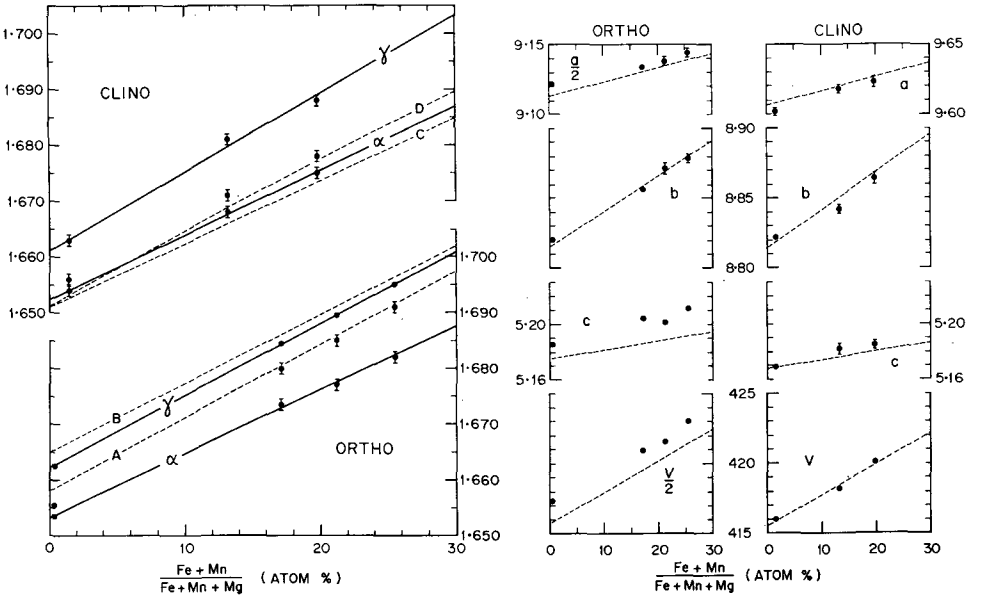

FIGS. 1 and 2: Fig. 1. Relationship between composition and refractive indices for the analysed Mg–Fe pyroxenes. The symbols denote accuracy of measurement for orthopyroxenes, and the range within which most measurements lie for clinopyroxenes. Line A (dashed) is a linear interpolation of γ between synthetic end member orthopyroxenes (Stephenson *et al.*, 1965; Lindsley *et al.*, 1964); B denotes γ for terrestrial orthopyroxenes after Deer *et al.*, 1963. C is a linear interpolation of α between synthetic clinopyroxenes (Winchell and Winchell, 1951, quoted by Stephenson *et al.*, 1966; Lindsley *et al.*, 1964), and curve D is α for synthetic clinopyroxenes after Bowen and Schairer, 1935. Fig. 2. Relationship between composition, cell parameters (Å), and cell volume (Å^3) for the analysed Mg–Fe pyroxenes. Symbols denote standard deviations derived by the method of Burnham (1962). The dashed lines represent values interpolated from those of synthetic end-members (Stephenson *et al.*, 1965; Burnham, 1965).

Several peaks in the pattern of the Château-Renard pyroxene are distorted or broadened and of diminished intensity, particularly 121, 511, 521, and 721. These features are probably related to the anomalous optical character of the orthopyroxene in this stone, and may reflect disorder caused by the shock responsible for the production of its maskelynite. The affected peaks do not conform to the rule for stacking disorder established by Pollack (1968), namely that $hk1$ reflections with h even are diffuse and those with h odd are sharp. The meteorites listed by Pollack as containing his type II disordered orthopyroxene are not maskelynite-bearing recrystallized stones

but rather Devitrified-primitive or Transitional Group chondrites showing limited recrystallization, in which conversion of monoclinic to orthorhombic Mg–Fe pyroxene is apparently incomplete (see below). Shock does not appear to have affected either the cell dimensions or the 10.3.1—060 spacing of the Château-Renard pyroxene, but it slightly lowers the precision of measurement.

Ca-*poor clinopyroxenes*

Chemistry. The analysed clinopyroxenes (table II) are notably richer in the minor constituents Al, Cr, Ca, Na, and K when compared to their orthorhombic equivalents, with the exception that the Kota-Kota clinoenstatite is poor in Ca (and possibly K) and has similar Al relative to the Hvittis enstatite. The two Fe-rich clinopyroxenes (strictly clinobronzite) contain slightly less Ti than their orthorhombic analogues, but the difference may not be significant. Ferric iron is again lacking or, in Kota-Kota, explainable by terrestrial oxidation.

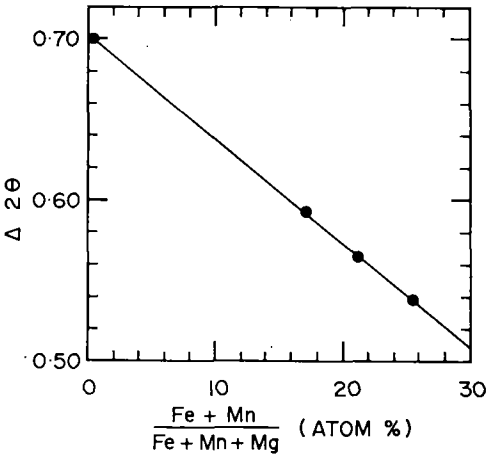

FIG. 3. Variation with composition of the angular spacing between the 10.3.1 and 060 reflections of chondritic orthopyroxenes (filtered Cu-$K\alpha$ radiation).

Ni once more appears too high to be due to metallic impurities and is apparently, at least in part, a genuine constituent of the pyroxenes. Although some Na and Al may be contained in vermicular inclusions (possibly exsolved during inversion from the proto form, see discussion below), their ratio does not satisfy the formula of a feldspar and both, certainly the latter, appear to be contained in the pyroxene structure.

All three clinopyroxenes are deficient in silica and contain an excess of divalent cations. In two cases this is partly due to olivine impurity, but sample contamination and analytical inaccuracies do not seem to offer sufficient explanation of the total discrepancy and there is a definite suggestion that the clinopyroxenes are slightly non-stoichiometric. The *Z*-site deficiency is accentuated if the cation contents listed in table II are reconstructed to maintain the balance between valence charges, for it then appears necessary to asign some Al to the six-fold co-ordination site. The two clinobronzites evidently contain increased cosmochlore component relative to the orthopyroxenes, but in the Kota-Kota clinoenstatite Cr may be combined with tetrahedral Al.

Optical properties and cell dimensions. Figs. 1 and 2 show the refractive indices and cell dimensions of the clinopyroxenes to increase systematically with Fe + Mn content,

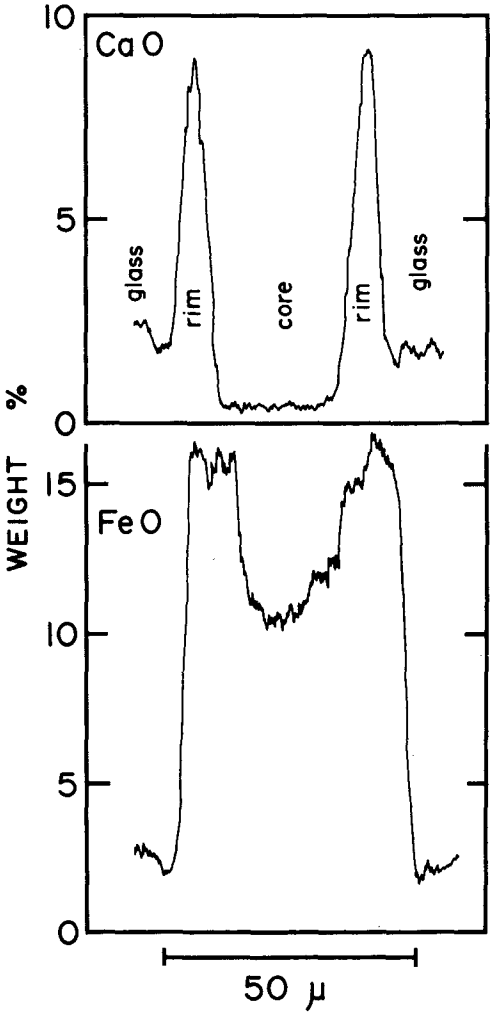

FIG. 4. Electron-probe profiles across a rimmed pyroxene phenocryst from a microporphyritic chondrule in the Parnallee meteorite (see also data in text). The core of twinned clinobronzite shows some Fe enrichment away from its centre, and is surrounded by a sharply defined untwinned rim of highly birefringent subcalcic 'augite' (probably low in Al_2O_3). The chondrule groundmass is red-brown glass. The scanning tracks for Ca and Fe were parallel but not coincident. Sloping boundaries in the profiles arise from probe diameter and fluorescence effects. Measurements elsewhere on the grain have shown that the peaks in the Ca profile depict the true Ca content of the rim pyroxene.

and to conform closely with those of synthetic equivalents. The refractive index α, measured across (100)-parting fragments, provides the best measure of composition.

Bowen and Schairer (1935) observed a linear relationship between refractive indices of synthetic members of the clinoenstatite–clinoferrosilite series and their weight % content of $FeSiO_3$. This implies a non-linear correlation on an atom %

basis, which possibly reflects the non-stoichiometry referred to above. Unfortunately the data presented here are neither sufficiently accurate nor abundant to establish a definite curvature in fig. 1.

The optic axial angles calculated from refractive index measurements, $2V_\gamma \approx 55°$ with optic axial plane $\perp$ (010), do not vary significantly with composition. They are substantially higher than the values of 20 to 25° given by Bowen and Schairer (1935), but agree with those listed by Atlas (1952) for synthetic clinoenstatite and by Dallwitz *et al.* (1966) and Trommsdorff and Wenk (1968) for terrestrial equivalents. The extinction angles increase with Fe+Mn content, and compare well with those given by Bowen and Schairer (1935).

Since data for pigeonite suggest that entry of Ca into the $P2_1/c$ pyroxene structure leads to substantial increase in a and c (Kuno and Hess, 1953; Morimoto *et al.*, 1960; Morimoto and Güven, 1967), it is perhaps surprising that the cell dimensions of chondritic clinopyroxenes correspond so closely to those of the synthetic clinoenstatite–clinoferrosilite series. Compensatory effects of other components, especially Al and Cr, must be assumed, and these possibly also explain the slightly lower monoclinic cell angle β of the chondritic samples.

The presence of small amounts of orthopyroxene in all three analysed clinopyroxenes is indicated by assymmetry on diffractometer traces of the 021 peak towards low 2θ, of 221 towards high 2θ, and also by very weak extra reflections at d 2·83, 2·71, and 2·48. The contamination is significant only in the Ghubara pyroxene, where about 10 % of untwinned orthopyroxene (partly xenocrystal, but partly related to the near-equilibration of the host portion of this stone, see Binns, 1968) may be observed in grain mounts. Certain Ghubara clinobronzite peaks also show broadening and diminished intensity, 221 in particular being almost absent. These anomalies may also reflect disorder due to shock, a suggestion supported by the relatively low intensity of the 521 reflection of the orthopyroxene contaminant at d 2·48 (see discussion of Château-Renard above).

Ca-*rich clinopyroxenes*

During electron probe studies connected with other projects, minor amounts of Ca-rich clinopyroxene have been encountered in several ordinary chondrites. As a more comprehensive study is being undertaken by W. R. Van Schmus, only a brief discussion is presented here.

In glassy-primitive chondrites, highly birefringent untwinned clinopyroxene occurs as microlites and as sharply distinguished rims surrounding clinobronzite–clinohypersthene phenocrysts in certain, presumably Ca-rich, chondrules. Electron-probe data for an example in Parnallee (see fig. 4) gave:

						Atoms %		
	SiO_2	FeO	MgO	CaO	Sum	Ca	Mg	Fe
Core	57·7	10·5	29·4	0·3	97·9	0·6	82·7	16·6
Rim	53·4	15·7	17·0	9·0	95·1	19·9	52·7	27·4

The rim, a comparatively iron-rich subcalcic 'augite', is similar in composition to a crystallite in a chondrule from the Chainpur chondrite described as 'pigeonite' by Fredriksson and Reid (1965).

In recrystallized chondrites, birefringent diopside occurs as platelets between orthopyroxene grains, especially within relic excentroradial chondrules, and very occasionally as rims about relic orthopyroxene phenocrysts in the remnants of microporphyritic chondrules. The former type of occurrence appears to have been derived by exsolution during the recrystallization process, for Ca-rich pyroxene is generally lacking in the excentroradial chondrules (containing clinoenstatite–clinohypersthene) of highly primitive chondrites. The diopsidic platelets themselves possess exceedingly fine (001) exsolution lamellae. Data for coexisting Ca-rich clinopyroxene and Ca-poor orthopyroxene from five recrystallized chondrites are presented in table IV.

TABLE IV. *Composition of coexisting pyroxenes in recrystallized chondrites, based on electron-probe microanalyses*

		Moti-ka-nagla	Oakley	Tauq	Peetz	Appley Bridge
Ca-rich clinopyroxene						
Atom %	Ca	44·4	44·7	44·5	44·7	44·0
	Mg	48·8	48·8	47·4	47·0	46·0
	Fe	6·8	6·5	8·1	8·3	10·0
Ca-poor orthopyroxene						
Atom %	Ca	1·5	1·7	1·7	1·6	1·8
	Mg	82·1	81·4	78·0	77·3	73·0
	Fe	16·4	16·9	20·3	21·1	25·2
Distribution coefficient						
	K_D	1·42	1·53	1·52	1·55	1·59

Genetic aspects of chondritic pyroxenes

Two outstanding problems in meteoritics are those concerning the origin of chondrules, and the significance of the mineralogical, textural, and compositional variation observed within each non-carbonaceous chondrite class. Both subjects are controversial, but before discussing the genetic significance of pyroxenes it is desirable to restate the stand adopted here in relation to the second.

Within each chemical-mineralogical class, the Devitrified-Primitive, Transitional, and Recrystallized Group chondrites (Binns, 1967*a*; effectively Van Schmus–Wood Types 4–6) are believed to have been derived by some kind of metamorphic process from material essentially equivalent to the corresponding Glassy-Primitive Group (Type 3) representatives. That is, progressive obliteration of chondritic textures, mineralogical changes including 'equilibration' of ferromagnesian silicates, and depletion in certain 'volatile' trace constituents are visualized as responses to post-accumulational events, rather than as a reflection of differing conditions during accretion or accumulation of chondritic material either directly or indirectly from the

presumed primordial solar nebula (cf. especially Larimer and Anders, 1967; Reid and Fredriksson, 1967; Blander and Abdel-Gawad, 1969). A detailed discussion of this interpretation is given by Dodd (1969) and further petrographic evidence in its favour will be presented elsewhere.

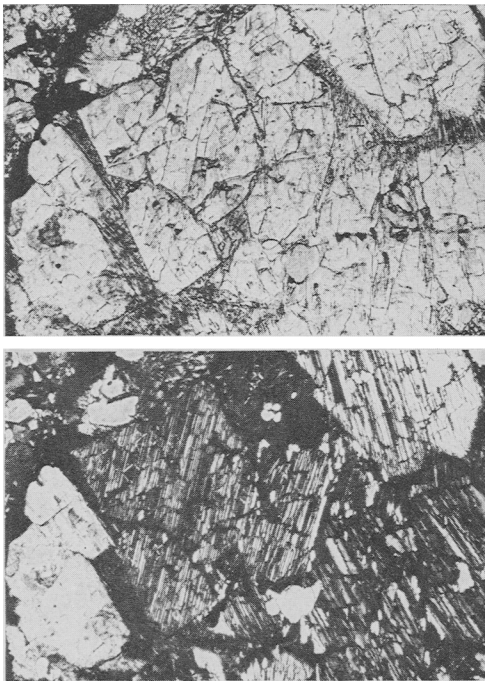

FIG. 5. Photomicrographs (ordinary light and crossed polars) of portion of a microporphyritic chondrule in the highly primitive Ngawi chondrite. Large euhedral clinobronzite phenocrysts show fine (100) polysynthetic twinning. Using inclination of composition planes, and extinction angle and birefringence of twin lamellae, as guides to orientation, the habit appears to be orthorhombic (proto?) rather than monoclinic. The crystal immediately left of centre, close to an (010) section, shows well-developed {*hol*} dome faces. That on the left, cut close to (100), shows {001} and {010} pinacoid, and {0*kl*} dome faces. The groundmass is dominantly glass with some birefringent microlites. Small anhedra of olivine (mainly white on the lower photograph) are enclosed by some pyroxene phenocrysts. Magnification × 90.

The high-temperature origin of chondrules. If the above viewpoint is accepted, evidence relating to the formation of chondrules must clearly be sought in the highly primitive, unequilibrated chondrites. The presence in these of fresh primary glass within many types of chondrule favours the quenched liquid droplet hypothesis for chondrule genesis (Sorby, 1864, 1867; Dodd and Van Schmus, 1965; Fredriksson and Reid, 1965). Crystallization of chondrules at near-liquidus temperatures is further indicated by the nature of their constituent pyroxene. In primitive stones such as Kota-Kota and Parnallee, much of the pyroxene (particularly that making up the analysed concentrates) is contained as phenocrysts, especially in microporphyritic chondrules of the type illustrated in fig. 5.

X-ray data presented in table III show these phenocrysts to be isostructural with the clinoenstatite polymorph of $MgSiO_3$. They are characterized in thin section by closely spaced (100) polysynthetic twinning and commonly by irregular 'shrinkage' partings normal to their *c* axes. When euhedrally developed, they often display terminations with apparently orthorhombic dome and pinacoid faces, some of which may be curved (see fig. 5 and also Binns, 1967*c*, fig. 1A). Such features, together with the presence of interstitial glass, indicate that the clinoenstatite–clinobronzite was formed by inversion from the high-temperature proto polymorph during comparatively rapid cooling (Boyd and England, 1965; cf. also Dallwitz *et al.*, 1966) rather than by deformation of pre-existing orthorhombic enstatite–bronzite (cf. Turner *et al.*, 1960; Trommsdorff and Wenk, 1968) or by direct crystallization within

the low-temperature field of the monoclinic Mg–Fe polymorph (cf. Sclar *et al.*, 1964; Boyd and England, 1965).

Evidence afforded by fragmented, indented, and composite chondrules indicates that their crystallization was in progress or even completed prior to final accumulation from a dispersed state, and hence that it took place at very low pressures, probably less than 1 atmosphere. Furthermore, the absence of hydrous minerals and the paucity of H_2O+ in primitive chondrites implies crystallization of chondrules under dry conditions. The crystallization temperatures of protoenstatite-bearing chondrules may therefore be placed within the range 1000–1560 °C on the basis of low-pressure experimental studies of polymorphism and melting in $MgSiO_3$ (Foster, 1951; Atlas, 1952; Boyd and Schairer, 1964; Boyd and England, 1965). The effects of the limited Fe and Ca substitution in chondritic pyroxenes are likely to be small compared to the over-all range quoted (cf. Bowen and Schairer, 1935; Boyd and Schairer, 1964; Lindsley, 1965). A temperature within this range is also implied by the composition of the calcic rims on the zoned Parnallee phenocrysts described in fig. 4. The rims clearly crystallized after the clinobronzite cores and the association is presumably not an equilibrium one, nevertheless a minimum temperature is set by the Ca content of the outer subcalcic 'augite'. Experimental studies of the immiscibility gap between Ca-rich and Ca-poor pyroxenes (Boyd and Schairer, 1964; Davis and Boyd, 1966; Green and Ringwood, 1967*a*; Bultitude and Green, 1968) suggest that temperatures exceeding *c.* 1200 °C are necessary to permit crystallization of Ca-rich pyroxene with the composition of the Parnallee rims.

These temperature estimates lie within the probable liquidus range of typical pyroxene-bearing chondrules (cf. Mason, 1968), and are incompatible with many genetic hypotheses for chondrules (see reviews by Wood, 1963; Anders, 1964; Ringwood, 1965). They constitute boundary conditions that must be satisfied by theories invoking creation of chondrules by direct or indirect condensation from the solar nebula (cf. Whipple, 1966; Larimer and Anders, 1967; Blander and Abdel-Gawad, 1969). Supercooling no doubt plays an important role in development of the curious internal structures of chondrules (Blander and Abdel-Gawad, 1969), but the former proto structure of pyroxenes in highly primitive chondrites limits the possible degree of undercooling during the earlier stages of chondrule formation.

The lack of ferric iron in the analysed Mg–Fe clinopyroxenes implies comparatively reduced conditions during crystallization. Before their accumulation, chondrules or their parent liquids may not necessarily have been closely associated with nickel-iron (cf. Urey and Craig, 1953), but even if they were, an observation by Bowen and Schairer (1935)—that silicate liquids contain some trivalent iron when in equilibrium with Fe metal under normal atmospheric conditions—suggests that pyroxenes crystallized from an ancestral chondrule melt might contain detectable Fe^{3+} unless buffered by a highly reduced gaseous phase (e.g. H_2).

Pyroxenes and the recrystallization of chondrites. The nature of the pyroxenes in most Devitrified Primitive and many Transitional Group chondrites, i.e. varieties intermediate between the two extreme types from which pyroxene concentrates have been

obtained, lends strong support to the metamorphic interpretation of the chondrite textural range. Although giving the X-ray powder diffraction pattern of orthopyroxene, these commonly show a striated appearance resembling clinoenstatite twinning when examined with the aid of a universal stage, but their 'composition planes' are less sharply defined and the maximum extinction angles are noticeably lower (from *c.* 15° to 3°, with a tendency to decrease with increasingly recrystallized appearance of the host stones) than in genuine clinoenstatite. Under 'flat stage' examination the structure may appear only as an undulose extinction if the 'composition planes' are at low inclination to the section. Orthopyroxene of this type in the Barwell meteorite has an anomalous positive optic axial angle (Jobbins *et al.*, 1966). Among meteorites listed by Pollack (1968), possession of striated orthopyroxene shows good correlation with type II structural disorder, whereas stacking order is more characteristic of normal orthopyroxene in highly recrystallized chondrites. The rare orthopyroxenes found in highly primitive chondrites (e.g. the contaminants in the clinopyroxene concentrates mentioned earlier in this article), if not xenocrystal, are generally of the striated type.

The above observations suggest that pyroxenes in equilibrated chondrites crystallized initially as the protoenstatite-type polymorph, inverted to the twinned clinoenstatite form during cooling, and then altered to (disordered?) orthopyroxene with relic twinning or to (ordered?) untwinned orthopyroxene depending on the intensity (temperature or duration) of recrystallization. Not only do they favour the metamorphic model for equilibrated chondrites, but they indicate recrystallization by reheating of a quenched clinoenstatite-bearing assemblage rather than during prolonged or arrested cooling of protoenstatite-bearing chondrites through the orthopyroxene stability field. These conclusions necessarily imply a more complex evolutionary history for the parent bodies of chondritic meteorites (cf. Dodd, 1969).

Physical conditions during recrystallization. Whatever the recrystallization process, the temperatures represented by silicate assemblages in the most thoroughly recrystallized kinds of ordinary (i.e. H, L, and LL groups) chondrite are reasonably well fixed both by the partition of Fe and Mg (Van Schmus and Koffman, 1967), and by the mutual miscibility relationship (Binns, 1967*a*) between coexisting orthopyroxene and Ca-rich clinopyroxene. Data listed in table IV give an average distribution coefficient

$$K_D = (\mathrm{Fe/Mg})_{opx}.(\mathrm{Mg/Fe})_{cpx}$$

of 1·52, intermediate between average values for terrestrial granulite facies metamorphic pyroxenes (1·78) and pyroxenes from 'dry' stratiform tholeiitic intrusives (1·35; data mainly from Kretz, 1963). A temperature between those represented by terrestrial igneous and metamorphic pyroxene pairs is indicated. A similarly intermediate relationship for the Ca-rich limit of the pyroxene solvus is implied by the composition of chondritic diopsidic clinopyroxenes (fig. 6). Hydrothermal experiments place granulite facies recrystallization temperatures in the 750–850 °C range (Binns, 1969), somewhat higher than earlier estimates, and the crystallization temperature of igneous pyroxene pairs may be taken as 1000–1150 °C (cf. Yoder and

Tilley, 1962) making some allowance for possible depression by hydrous conditions. Assuming that pressure effects are negligible (Kretz, 1963; Davis and Boyd, 1966), these figures indicate a temperature of *c.* 900 to 950 °C, within the orthopyroxene stability field (Boyd and England, 1965; Lindsley, 1965), for the pyroxene assemblages in thoroughly recrystallized ordinary chondrites.

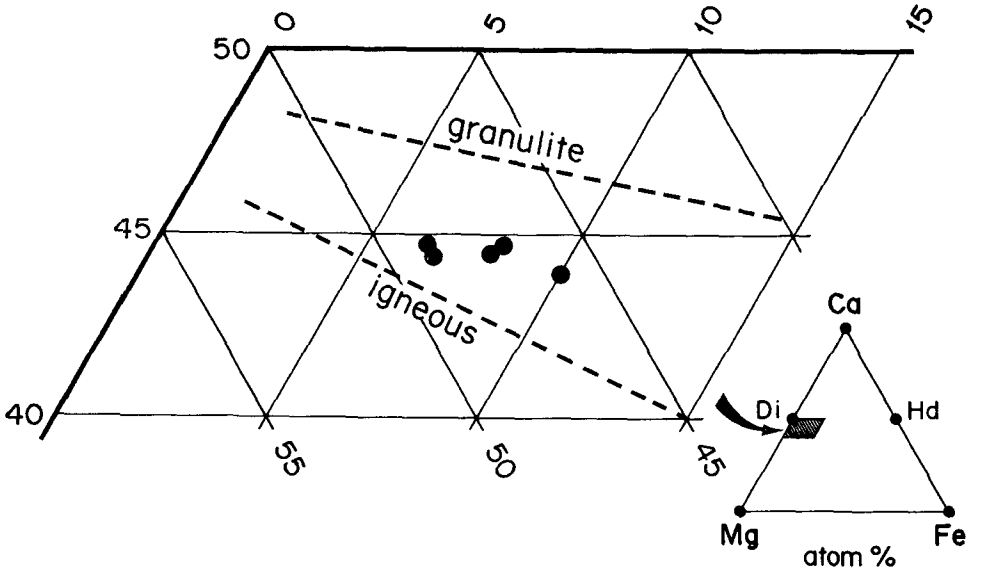

FIG. 6. Composition of Ca-rich clinopyroxenes in five recrystallized chondrites (Table IV), plotted on the diopsidic portion of the pyroxene quadrilateral (see key at lower right). The chondritic pyroxenes lie part-way between the trends for terrestrial basic igneous and granulite facies metamorphic clinopyroxenes that coexist with Ca-poor pyroxene (after Binns, 1965, fig. 3*b*).

Recrystallized enstatite chondrites are not known to contain calcium-rich pyroxene, but their possession of almost pure orthoenstatite and accessory tridymite (Binns, 1967*b*) defines temperatures of the same order. Taking the *P–T* relationships of Tuttle and Bowen (1958) for the quartz–tridymite inversion and of Boyd and England (1965) for the orthoenstatite–protoenstatite inversion, coexistence of these two minerals is restricted to pressures below *c.* 1 kb and to temperatures from *c.* 870 to 1060 °C (870 to 985 °C at pressures close to 1 atm).

Mineralogical indications of pressure in recrystallized ordinary chondrites are far less definitive. From a broad extrapolation of experimental data on olivine tholeiite (Green and Ringwood, 1967*b*), the absence of jadeite-rich pyroxene and pyrope-rich garnet from chondritic assemblages delineates a maximum limit of *c.* 10 kb for temperatures of 900 to 950 °C. The analysed chondritic orthopyroxenes contain less Al than most terrestrial igneous and metamorphic orthopyroxenes coexisting with plagioclase, but although suggestive of very low pressures, appropriate experimental data are scarce (cf. Boyd and England, 1960). Investigation of any jadeite component in

chondritic Ca-rich clinopyroxene may provide a better indication of pressure during recrystallization.

If, indeed, recrystallized chondrites were formed in response to rising temperatures rather than during slow cooling, the remarkable homogeneity of their ferromagnesian silicate phases suggest that the above estimates represent values close to the peak temperatures attained, particularly those based on the composition of Ca-rich clinopyroxenes, whose very fine exsolution lamellae, developed during subsequent cooling, were not resolved by the electron probe. There are certain indications that the texturally less altered Devitrified-Primitive and Transitional Group chondrites reached lower peak temperatures than the Recrystallized Group chondrites discussed above. In ordinary chondrites, Dodd (1969) has observed a slight increase in Ca content of orthopyroxene from petrologic type 4 to type 6 chondrites, suggesting contraction of the pyroxene immiscibility gap at successively higher recrystallization temperatures. Several chondrites of intermediate textural type examined by the writer contain diopsidic platelets with higher Ca contents than those listed in table IV. Unfortunately the platelets are very narrow and the electron-probe data need refinement, but since it is unlikely that improved resolution will decrease the apparent Ca contents, these preliminary measurements tend to substantiate Dodd's suggestion. Among enstatite chondrites, the only Transitional Group representative studied by the writer (St. Mark's) contains orthoenstatite accompanied by quartz rather than tridymite, which suggests either lower temperature or higher pressure during recrystallization compared to Recrystallized Group enstatite chondrites such as Hvittis. If lower temperatures can be conclusively demonstrated for stones with less-altered textural appearances, the reheating rather than a prolonged cooling model for chondritic recrystallization will have been established almost beyond doubt.

Chemical changes in pyroxenes during recrystallization. Assuming the analysed concentrates to be representative of the two extreme textural kinds of chondrite, the inversion of Mg–Fe pyroxene from monoclinic to orthorhombic symmetry during recrystallization is not strictly isochemical. It is accompanied firstly by elimination of variations in Mg/Fe content within zoned clinoenstatite crystals and between pyroxenes in different chondrules. This 'equilibration' also affects olivine, but in the pyroxenes it is presumably aided by the presence of fine polysynthetic twin lamellae and by the structural rearrangements associated with inversion. Data listed in table II show that minor element concentrations also change during inversion, and this will have some influence on final mineral assemblages in recrystallized chondrites.

The comparatively reduced enstatite chondrites must be considered separately, for it is clear that sulphide minerals are involved in the over-all chemical balance (cf. Keil, 1968). The Kota-Kota and Hvittis pyroxenes suggest that Fe, Mn, and Cr have been rejected to sulphides including alabandine and daubréelite (chromite is unknown in enstatite chondrites), while Ca and possibly K have been taken up from other phases. The potassium may come from djerfisherite, but the source of calcium is less clear. Oldhamite and niningerite are potential Ca donors, although the modal data of Keil (1968) do not indicate sufficiently great differences in content of these minerals

between primitive (his Type I) and recrystallized (Type II) enstatite chondrites respectively to explain the observed Ca content of the Hvittis enstatite. As shown by Keil, the Na and Al contents of clinoenstatite and orthoenstatite are too close to explain the abundance of sodic plagioclase in recrystallized enstatite chondrites (Mason, 1966).

In ordinary chondrites, the change from monoclinic to orthorhombic pyroxene involves loss of Ca, Cr, Al, and alkalis. Calcium would be contributed to the platelets of diopsidic pyroxene commonly associated with orthopyroxene in recrystallized chondrites, and chromium is probably expelled to the 'exsolution' chromite described by Ramdohr (1963). Chromite is a primary constituent of unequilibrated chondrites, but is probably more abundant in recrystallized chondrites (Dodd, 1969). From normative calculations of average pyroxene abundances in ordinary chondrites, it appears that approximately a quarter of the total chromite in recrystallized ordinary chondrites would be released by the pyroxene inversion. The Al and alkalis expelled from clinopyroxenes during inversion to orthopyroxene presumably crystallize as feldspar, but the respective differences are such that only about 5 % of the sodic plagioclase in recrystallized ordinary chondrites could arise in this way. The remainder derives largely from recrystallization of original chondrule glass (cf. Mason, 1965, 1967*b*).

Concluding remarks. Several aspects of this study are pertinent to investigations of terrestrial pyroxenes. It has been noted that the analysed chondritic clinoenstatites and clinobronzites may be slightly non-stoichiometric. This feature would be inherited from protoenstatite-structured ancestors, and it may need to be taken into account in experimental studies of pyroxene polymorphism. Data relating to the extent of Fe substitution possible in the protoenstatite structure are also provided by the refractive index range of the clinopyroxene concentrates. The maximum value observed for twinned clinopyroxene in Parnallee (1·695) suggests the former stability of protohypersthene containing at least 24 mol % $(Fe,Mn)SiO_3$ (fig. 1). Electron probe analyses presented in histogram form by Dodd *et al.* (1967) extend to slightly more than 40 mol % ferrosilite, but the monoclinic symmetry of these iron-rich pyroxenes has not been confirmed. Finally, it may be noted that the striated structure of orthopyroxene in certain chondrites of intermediate textural aspect resembles the lamellar twinning described by Henry (1942). It would be interesting to investigate the possibility that twinned terrestrial orthopyroxenes also crystallized initially as protopyroxene.

Acknowledgements. The writer is grateful to the staff of the British Museum (Natural History) for their assistance with this investigation, most particularly to Mr. A. J. Easton for his careful microanalyses, Dr. S. J. B. Reed for help with electron probe studies, and Dr. M. H. Hey for provision of the meteorite samples.

REFERENCES

ANDERS (E.), 1964. *Space Sci. Rev.* **3**, 583.
ATLAS (L.), 1952. *Journ. Geol.* **60**, 125 [M.A. **12**–80].
BINNS (R. A.), 1965. *Min. Mag.* **35**, 561 [M.A. **17**–634].
—— 1967*a*. *Earth Planet. Sci. Lett.* **2**, 23.
—— 1967*b*. *Amer. Min.* **52**, 1549 [M.A. **19**–121].
—— 1968. *Geochimica Acta*, **32**, 299 [M.A. **19**–210].
—— 1969. *Hydrothermal Investigations of the Amphibolite–Granulite Facies Boundary*. Spec. Publ. Geol. Soc. Australia, **2**, 341–4.
BLANDER (M.) and ABDEL-GAWAD (M.), 1969. *Geochimica Acta*, **33**, 701.
BOWEN (N. L.) and SCHAIRER (J. F.), 1935. *Amer. Journ. Sci.* **229**, 151 [M.A. **6**–352].
BOYD (F. R.) and ENGLAND (J. L.), 1960. *Ann. Rep. Geophys. Lab. Carnegie Inst. Washington*, **59**, 47.
—— —— 1965. Ibid. **64**, 117.
—— and SCHAIRER (J. F.), 1964. *Journ. Petrology*, **5**, 275 [M.A. **17**–281].
BULTITUDE (R. J.) and GREEN (D. H.), 1968. *Earth Planet. Sci. Lett.* **3**, 325.
BURNHAM (C. W.), 1962. *Ann. Rep. Geophys. Lab. Carnegie Inst. Washington*, **61**, 132.
—— 1965. Ibid. **64**, 202.
DALLWITZ (W. B.), GREEN (D. H.), and THOMPSON (J. E.), 1966. *Journ. Petrology*, 7, 375 [M.A. **19**–134].
DAVIS (B. T. C.) and BOYD (F. R.), 1966. *Journ. Geophys. Res.* **71**, 3567 [M.A. **18**–21].
DEER (W. A.), HOWIE (R. A.), and ZUSSMAN (J.), 1963. *Rock-forming Minerals*, **2**. London (Longmans).
DODD (R. T.), 1969. *Geochimica Acta*, **33**, 161.
—— and VAN SCHMUS (W. R.), 1965. *Journ. Geophys. Res.* **70**, 3801 [M.A. **17**–491].
—— —— and KOFFMAN (D. M.), 1967. *Geochimica Acta*, **31**, 921 [M.A. **19**–299].
DUNDON (R. W.) and WALTER (L. S.), 1967. *Earth Planet. Sci. Lett.* **2**, 372.
FOSTER (W. R.), 1951. *Journ. Amer. Ceram. Soc.* **34**, 255 [M.A. **11**–470].
FREDRIKSSON (K.) and REID (A. M.), 1965. *Science*, **149**, 856.
GREEN (D. H.) and RINGWOOD (A. E.), 1967*a*. *Contr. Min. Petr.* **15**, 103.
—— —— 1967*b*. *Geochimica Acta*, **31**, 767 [M.A. **18**–170].
HENRY (N. F. M.), 1942. *Min. Mag.* **26**, 179.
HESS (H. H.), 1952. *Amer. Journ. Sci.*, Bowen vol., 173 [M.A. **12**–97].
JOBBINS (E. A.), DIMES (F. G.), BINNS (R. A.), HEY (M. H.), and REED (S. J. B.), 1966. *Min. Mag.* **35**, 881 [M.A. **18**–36].
KEIL (K.), 1968. *Journ. Geophys. Res.* **73**, 6945.
—— and FREDRIKSSON (K.), 1964. Ibid. **69**, 3487 [M.A. **17**–173].
KRETZ (R.), 1963. *Journ. Geol.* **71**, 773 [M.A. **17**–195].
KUNO (H.) and HESS (H. H.), 1953. *Amer. Journ. Sci.* **251**, 741 [M.A. **12**–334].
LARIMER (J. W.) and ANDERS (E.), 1967. *Geochimica Acta*, **31**, 1239 [M.A. **19**–120].
LIBERMANN (A.), 1955. *Analyst*, **80**, 595 [M.A. **13**–75].
LINDSLEY (D. H.), 1965. *Ann. Rep. Geophys. Lab. Carnegie Inst. Washington*, **64**, 148.
—— MACGREGOR (I. D.), and DAVIS (B. T. C.), 1964. Ibid. **63**, 174.
MASON (B.), 1962. *Amer. Museum Novitates*, no. 2085, 20 pp. [M.A. **16**–639].
—— 1963. *Geochimica Acta*, **27**, 1011 [M.A. **16**–449].
—— 1965. *Science*, **148**, 943 [M.A. **18**–112].
—— 1966. *Geochimica Acta*, **30**, 23 [M.A. **18**–36].
—— 1967*a*. Ibid. **31**, 1100 [M.A. **19**–299].
—— 1967*b*. *Amer. Min.* **52**, 307 [M.A. **18**–270].
—— 1968. *Lithos*, **1**, 1 [M.A. **19**–299].
MORIMOTO (N.), APPLEMAN (D. E.), and EVANS (H. T.), 1960. *Zeits. Krist.* **114**, 120 [M.A. **15**–96].
—— and GÜVEN (N.), 1967. *Ann. Rep. Geophys. Lab. Carnegie Inst. Washington*, **66**, 494.
MOSS (A. A.), HEY (M. H.), and BOTHWELL (D. I.), 1961. *Min. Mag.* **32**, 802 [M.A. **15**–247].
POLLACK (S. S.), 1968. *Geochimica Acta*, **32**, 1209 [M.A. **20**–136].
PRIOR (G. T.), 1920. *Min. Mag.* **19**, 51.
RAMDOHR (P.), 1963. *Journ. Geophys. Res.* **68**, 2011 [M.A. **17**–57].
REID (A. M.) and COHEN (A. J.), 1967. *Geochimica Acta*, **31**, 661 [M.A. **19**–299].
—— and FREDRIKSSON (K.), 1967. *In* ABELSON (P. H.), (*ed.*), *Researches in Geochemistry*, **2** New York (Wiley) [M.A. **19**–87].

RILEY (J. P.), 1958. *Anal. Chim. Acta*, **19**, 413 [M.A. **14**–87].
—— and WILLIAMS (H. P.), 1959. *Mikrochim. Acta*, 516 [M.A. **14**–316].
RINGWOOD (A. E.), 1965. *Rev. Geophys.* **4**, 113.
SCLAR (C. B.), CARRISON (L. C.), and SCHWARTZ (C. M.), 1964. *Trans. Amer. Geophys. Union*, **45**, 121.
SHAPIRO (L.) and BRANNOCK (W. W.), 1962. *U.S. Geol. Surv. Bull.* 1144-A, 56 pp.
SMITH (J. V.), STEPHENSON (D. A.), HOWIE (R. A.), and HEY (M. H.), 1969. *Min. Mag.* **37**, 90.
SORBY (H. C.), 1864. *Proc. Roy. Soc.* **13**, 333.
—— 1877. *Nature*, **15**, 495.
STEPHENSON (D. A.), SCLAR (C. B.), and SMITH (J. V.), 1965. *Min. Mag.* **35**, 838 [M.A. **17**–658].
THIEL (A.) and PETER (O.), 1935. *Zeits. anal. Chemie*, **103**, 161.
TROMMSDORFF (V.) and WENK (H.-R.), 1968. *Contrib. Min. Petr.* **19**, 158.
TURNER (F. J.), HEARD (H.), and GRIGGS (D. T.), 1960. *Rept. 21st Int. Geol. Congress, Norden*, **18**, 399
TUTTLE (O. F.) and BOWEN (N. L.), 1958. *Mem. Geol. Soc. Amer.* **74**, 153 pp. [M.A. **14**–89].
UREY (H. C.) and CRAIG (H.), 1953. *Geochimica Acta*, **4**, 36 [M.A. **12**–242].
VAN SCHMUS (W. R.) and KOFFMAN (D. M.), 1967. *Science*, **155**, 1009.
—— and WOOD (J. A.), 1967. *Geochimica Acta*, **31**, 747 [M.A. **19**–120].
WINCHELL (A. N.) and WINCHELL (H.), 1951. *Elements of Optical Mineralogy*, Part II. *Descriptions of Minerals*, 4th edn. New York (Wiley) [M.A. **11**–463].
WOOD (J. A.), 1963. In *The Solar System IV*, MIDDLEHURST (B. M.) and KUIPER (G. P.) (*eds.*) Chicago (University of Chicago Press).
YODER (H. S.) and TILLEY (C. E.), 1962. *Journ. Petrology*, **3**, 342 [M.A. **16**–475].
ZWAAN (P. C.), 1954. *Leidse Geol. Medelingen*, **19**, 167 [M.A. **13**–531].

[*Manuscript received 4 July 1969*]